

# A Combinatorial Library of Lipid Nanoparticles for RNA Delivery to Leukocytes

Srinivas Ramishetti, Inbal Hazan-Halevy, Ramesh Palakuri, Sushmita Chatterjee, Somu Naidu Gonna, Niels Dammes, Inbar Freilich, Luba Kolik Shmuel, Dganit Danino, and Dan Peer\*

Lipid nanoparticles (LNPs) are the most advanced nonviral platforms for small interfering RNA (siRNA) delivery that are clinically approved. These LNPs, based on ionizable lipids, are found in the liver and are now gaining much attention in the field of RNA therapeutics. The previous generation of ionizable lipids varies in linker moieties, which greatly influences in vivo gene silencing efficiency. Here novel ionizable amino lipids based on the linker moieties such as hydrazine, hydroxylamine, and ethanolamine are designed and synthesized. These lipids are formulated into LNPs and screened for their efficiency to deliver siRNAs into leukocytes, which are among the hardest to transfect cell types. Two potent lipids based on their in vitro gene silencing efficiencies are also identified. These lipids are further evaluated for their biodistribution profile, efficient gene silencing, liver toxicity, and potential immune activation in mice. A robust gene silencing is also found in primary lymphocytes when one of these lipids is formulated into LNPs with a pan leukocyte selective targeting agent ( $\beta_7$  integrin). Taken together, these lipids have the potential to open new avenues in delivering RNAs into leukocytes.

RNA interference (RNAi) is a prominent and natural cellular process for understanding gene function in many cell types.<sup>[1]</sup> Taking advantage of this process, specific genes can be downregulated by intracellular delivery of synthetic small interfering RNA (siRNA) and micro RNA (miRNA) molecules.<sup>[2]</sup> Once delivered to the cytoplasm, siRNA can load into the RNA-induced silencing complex (RISC) and direct

the sequence-specific cleavage of target mRNA.<sup>[3]</sup> However, siRNAs are unable to cross the cell membrane due to their poly-anionic nature, therefore suitable delivery strategies are required to access the target cell cytoplasm.<sup>[4–6]</sup> Nonviral gene therapy is the most promising strategy to deliver nucleic acids with less or no immunogenic responses compared to viral gene delivery.<sup>[7,8]</sup> Lipid nanoparticles (LNPs) containing ionizable amino lipids are the most advanced nonviral delivery platforms for negatively charged nucleic acids.<sup>[8–10]</sup> Ionizable amino lipid is a critical component of LNPs functionality. Structural changes during the interaction of ionizable amino lipids with endosomal membrane facilitate the endosomal escape of nucleic acid.<sup>[9]</sup> However, less than 2% of the loaded siRNAs are released from the endosomes with a surprisingly high efficiency of almost 100% gene silencing.<sup>[11]</sup>

The structure of ionizable lipids is divided into three major parts: hydrophilic amine head group, hydrophobic lipid chain, and a linker region that connects these two parts. The recently FDA-approved RNAi-based drug, Onpatro (Patisiran), is comprised of the amino lipid Dlin-MC3-DMA (MC3) as part of the LNP structure.<sup>[12]</sup> Despite being a promising candidate, unfavorable adverse effects hinder the use of MC3 for chronic therapies.<sup>[13]</sup> Predominant liver uptake of

Dr. S. Ramishetti, Dr. I. Hazan-Halevy, Dr. R. Palakuri, Dr. S. Chatterjee, Dr. S. Naidu Gonna, Dr. N. Dammes, Prof. D. Peer  
Laboratory of Precision NanoMedicine  
School of Molecular Cell Biology and Biotechnology  
George S. Wise Faculty of Life Sciences  
Tel Aviv University  
Tel Aviv 69978, Israel  
E-mail: peer@tauex.tau.ac.il

Dr. S. Ramishetti, Dr. I. Hazan-Halevy, Dr. R. Palakuri, Dr. S. Chatterjee, Dr. S. Naidu Gonna, Dr. N. Dammes, Prof. D. Peer  
Department of Materials Sciences and Engineering  
Faculty of Engineering  
Tel Aviv University  
Tel Aviv 69978, Israel

Dr. S. Ramishetti, Dr. I. Hazan-Halevy, Dr. R. Palakuri, Dr. S. Chatterjee, Dr. S. Naidu Gonna, Dr. N. Dammes, Prof. D. Peer  
Center for Nanoscience and Nanotechnology and Cancer Biology  
Research Center  
Tel Aviv University  
Tel Aviv 69978, Israel

I. Freilich, Dr. L. Kolik Shmuel, Prof. D. Danino  
CryoEM Laboratory of Soft Matter  
Faculty of Biotechnology and Food Engineering  
Technion  
Haifa 3200003, Israel

 The ORCID identification number(s) for the author(s) of this article can be found under <https://doi.org/10.1002/adma.201906128>.

DOI: 10.1002/adma.201906128

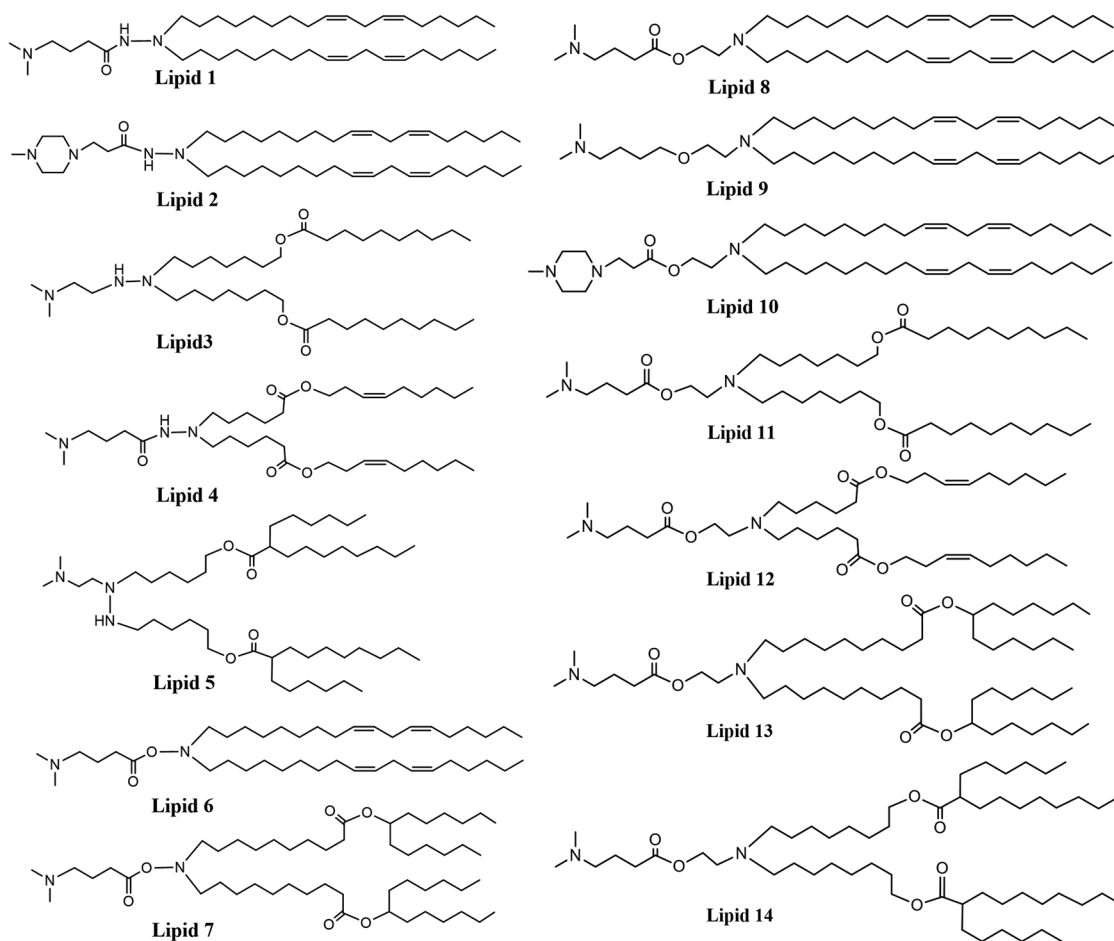


**Figure 1.** Chemical structures of the designed lipids.

these LNPs occurred due to apolipoprotein E (ApoE) binding in circulation followed by the uptake of liver cells via the low-density lipoprotein (LDL) receptors.<sup>[14]</sup>

Our objective was to design new lipid structures for siRNAs delivery that could be delivered beyond the liver in a safe manner. We specifically concentrated on designing new lipids for in vivo delivery of RNAi payloads into hard-to-transfect cells, such as leukocytes. Previous generations of active ionizable lipids vary only in the linker region, but greatly influenced the in vivo efficiency in hepatic cells.<sup>[8]</sup> To this end, using a rational approach, we designed a new class of amino lipid molecules containing hydrazine, hydroxylamine, or ethanolamine as a linker backbone. These linkers are easily available and simple synthetic procedures were needed for the modification. The lipid chain we have chosen is either a linoleic fatty acid chain, known to be optimal for activity<sup>[15]</sup> or a branched lipid chain that contains labile ester groups.<sup>[13]</sup> As the headgroups, we chose regular tertiary amine with single ionizable amine or piperazine head groups with two ionizable amine groups.

The newly synthesized lipids (**Figure 1**) were characterized by NMR and mass spectroscopy methods. LNPs made of these lipids, encapsulated siRNAs were screened for in vitro silencing efficiency, followed by their ability to downregulate gene expression in leukocyte populations upon systemic

administration into mice. Additionally, we have evaluated these new lipids (in the form of LNPs) for potential liver toxicity and immune system activation.

The structure of the new lipids is shown in **Figure 1**. All the lipids were synthesized using standard organic synthesis procedures (see Supporting Information) and characterized by NMR and mass spectroscopy (see Supporting Information). LNPs were composed of ionizable lipid, cholesterol, 1,2-distearoyl-sn-glycero-3-phosphocholine (DSPC), and PEGylated lipids in the molar ratios of 50:38.5:10:1.5, respectively, and assembled using a microfluidic mixing device, Nanoassembler, as previously reported.<sup>[16,17]</sup> The produced LNPs were small and uniformly distributed as evidenced by hydrodynamic diameter and polydispersity index (PDI). The mean size of LNPs was less than 100 nm in diameter with PDI less than 0.1 and the surface potential was almost neutral for most of the lipids composing the LNPs (**Figure 2a,b**). The cryo-electron microscopy analysis revealed that lipid 8 and lipid 10 composed-LNPs were about 50 nm in diameter, spherical, densely packed, and uniform, in agreement with the dynamic light scattering (DLS) data (**Figure 2c**). Interestingly, the size of LNPs with the branched lipids varies with linkers despite their similar branched hydrophobic moieties (**Figure 2a** and **Figure S1**, Supporting Information). This could be explained by the arrangement of lipid

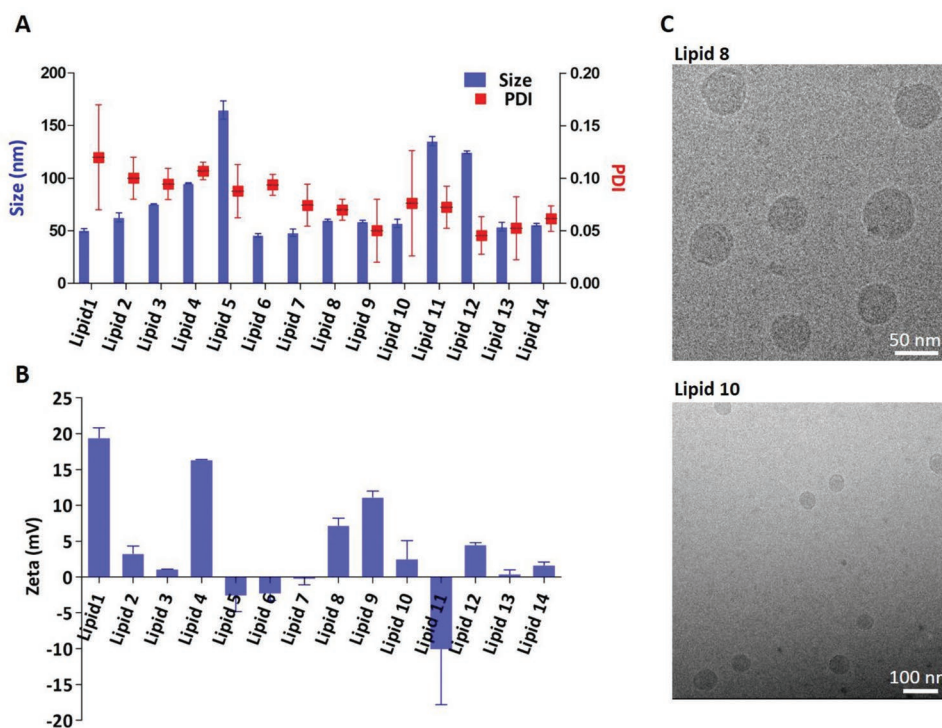


**Figure 2.** Physico-chemical properties of LNPs made from different ionizable lipids (lipids 1–14). a) LNPs mean diameter and PDI; b) zeta potential measured by Zeta Sizer; c) cryo-TEM analysis of lipid-8- and lipid-10-based LNPs.

tails during the LNPs assembly. LNPs based on lipids 6, 8, and 10 showed stability in medium with 10% and 50% serum for 24 h (Figure S10, Supporting Information).

Next, we entrapped polo-like kinase 1 (PLK1) siRNA into the LNPs and screened for their ability to silence gene expression and affect cell viability in U266 (multiple myeloma suspension cells). PLK1 is overexpressed in a variety of tumor types and has a significant role in the maintenance of mitotic integrity. The silencing of PLK1 will arrest the cell cycle leading ultimately to cell death.<sup>[17,18]</sup> The U266 cells were treated with different LNP-siPLK1 at a dose of 0.06  $\mu$ M and the cell viability was measured by the XTT assay. The lipid DLin-MC3-DMA-based LNPs served as a positive control. As shown in Figure 3a, the cell viability was reduced significantly after the treatment with lipid-2-, lipid-6-, lipid-8-, and lipid-10-based LNPs compared to other lipids, whereas LNPs containing negative control (NC) siRNAs did not affect the cell viability (Figure S2, Supporting Information). The dose-dependent effect of siPLK1 on the cell viability was measured for the lipid-8- and lipid-10-based LNPs (Figure 3b) and for the rest of the lipids (Figure S3, Supporting Information). LNPs containing siNC did not affect the cell viability, demonstrating the safe use of these lipids (Figure S4, Supporting Information). Interestingly, lipids having piperazine head groups (lipids 2 and 10) showed improved transfection efficiency compared to their tertiary amine head groups (lipids 1 and 8). Moreover, lipids that had a branched-chain with ester bonds were less effective than those having linoleic fatty acid chains. This could be attributed to a better endosomal escape due to the structural change of linoleic lipid in the endosomes.<sup>[11]</sup> Reduced PLK1-mRNA levels in U266 cells by LNPs-siPLK1 with lipids 8 or 10 (Figure 3c), was translated into a dose-dependent effect

on U266 cell viability and apoptosis (Figure 3d and Figure S5, Supporting Information). The uptake of LNPs based on lipids 2, 6, 8, and 10 by U266 cells was analyzed by confocal microscopy. In accordance with the above results, LNPs based on lipids 8 or 10 internalized more effectively into U266 cells compared to LNPs based on lipid 6. LNPs based on lipid 2 were mostly sticky to the cell membrane (Figure 3e).

Next, we examined the biodistribution of lipid-10-based LNPs in wild type mice. LNPs formulated with Cy5-labeled siRNA (siCy5) were administered intravenously and organs were harvested and analyzed 2 h and 24 h post-administration. As shown in Figure 4a,b, lipid-10-based LNPs mostly accumulated in the spleen compared to the liver at both time points. A vague fluorescent signal was observed in the liver after 24 h (Figure 4a,b). As opposed, lipid-8-based LNPs accumulated more in the liver than in the spleen (Figure S6, Supporting Information). To evaluate the linker effect on the LNPs biodistribution, we further tested the biodistribution of LNPs based on lipids 2 and 6 (Figure S7, Supporting Information). Interestingly, piperazine head group lipids (lipids 2 and 10) accumulated more in the spleen than the liver, whereas tertiary amine head group lipids (lipids 6 and 8) accumulated more in the liver than the spleen. Previous reports demonstrated that the biodistribution of liposomes is greatly influenced by changes in their surface potentials.<sup>[19]</sup> Nevertheless, our results demonstrate that headgroup moieties can influence the biodistribution profile of LNPs despite differences in surface potentials (Figure S8, Supporting Information).

Following the unique biodistribution profile of lipid-10-based LNPs to the spleen, we further focused on the potential of using lipid-10-based LNPs for in vivo silencing of primary lymphocytes.<sup>[16,20]</sup> We have previously shown that CD4-mAb conjugated

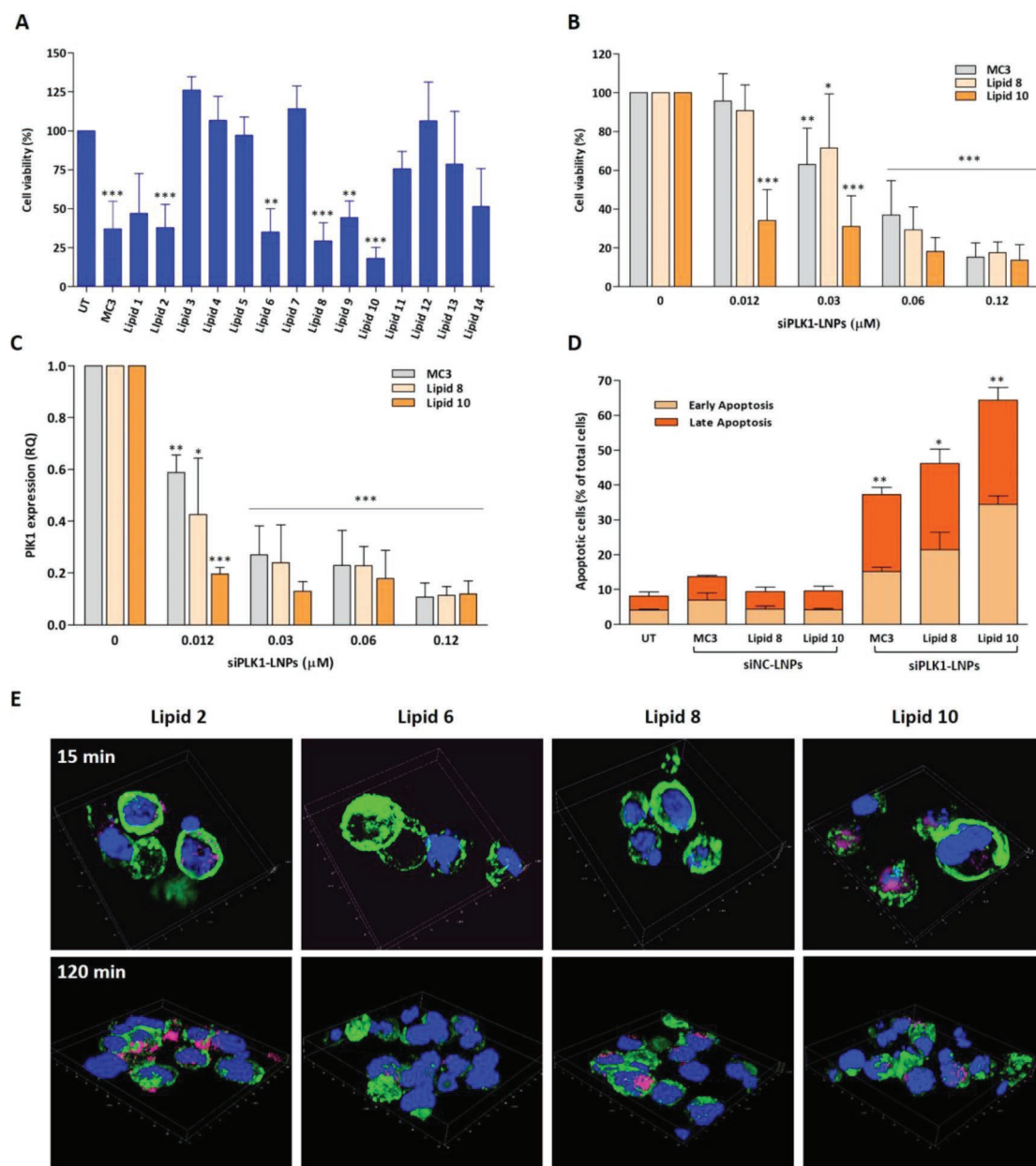


**Figure 3.** In vitro gene silencing efficiency in U266 multiple myeloma cells using LNP-siPLK1. U266 cells were incubated with LNP-siPLK1 for 72 h at different doses. a) The effect of LNP-siPLK1 on cell viability, measured by XTT assay; b) dose-dependent effect of MC3, lipid-8- or lipid-10-based LNP-siPLK1 on cell viability; c) dose-dependent effect of MC3, lipid-8- or lipid-10-based LNP-siPLK1 on PLK1-mRNA levels calculated by qPCR. d) The effect of MC3, lipid-8- or lipid-10-based LNP-siPLK1 or LNP-siNC ( $0.06 \times 10^{-6}$  M) on cell apoptosis analyzed by PI-Annexin. Results are average  $\pm$  SD from triplicate experiments, \* $p < 0.05$ , \*\* $p < 0.001$ , \*\*\* $p < 0.0001$  compared to untreated cells (two-sided student's t-test); e) confocal microscopy analysis of lipid-2-, lipid-6-, lipid-8-, and lipid-10-based LNP uptake, 15 min and 120 min post-LNP administration, by U266 cells. (Green: Alexa Fluor 488-CD44 for membrane staining; Blue: Hoechst for nucleus staining; Pink: siCy5 LNPs).

LNPs specifically target and silence gene expression in CD4<sup>+</sup> T lymphocytes in vivo.<sup>[16]</sup> Here, we have chosen an anti-integrin  $\beta_7$  mAb as a targeting moiety to facilitate the internalization of LNPs to both CD4<sup>+</sup> and CD8<sup>+</sup> T lymphocytes. LNPs were encapsulated with siCD45 to downregulate the stable pan leukocyte marker, CD45.<sup>[16,17]</sup> LNPs were surface modified with either an anti- $\beta_7$ -mAb (tLNPs) or isotype control LNPs (isoLNPs) via conventional thiol-maleimide reaction (Figure 4c). As shown in Figure 4d-f, tLNPs-siCD45 demonstrated significant

downregulation of CD45 expression in both CD4<sup>+</sup> and CD8<sup>+</sup> T lymphocytes, whereas isoLNPs had no effect. We observed CD45 silencing more robustly in lymph nodes compared to that of splenic lymphocytes (Figure 4d), additionally silencing was higher in CD8<sup>+</sup> T-lymphocytes (Figure 4f) compared to CD4<sup>+</sup> T-lymphocytes (Figure 4e) in both spleen and inguinal lymph nodes. However, the silencing observed is limited, as we previously reported, tLNPs are internalized only in part of the lymphocyte population. We have also shown that the silencing

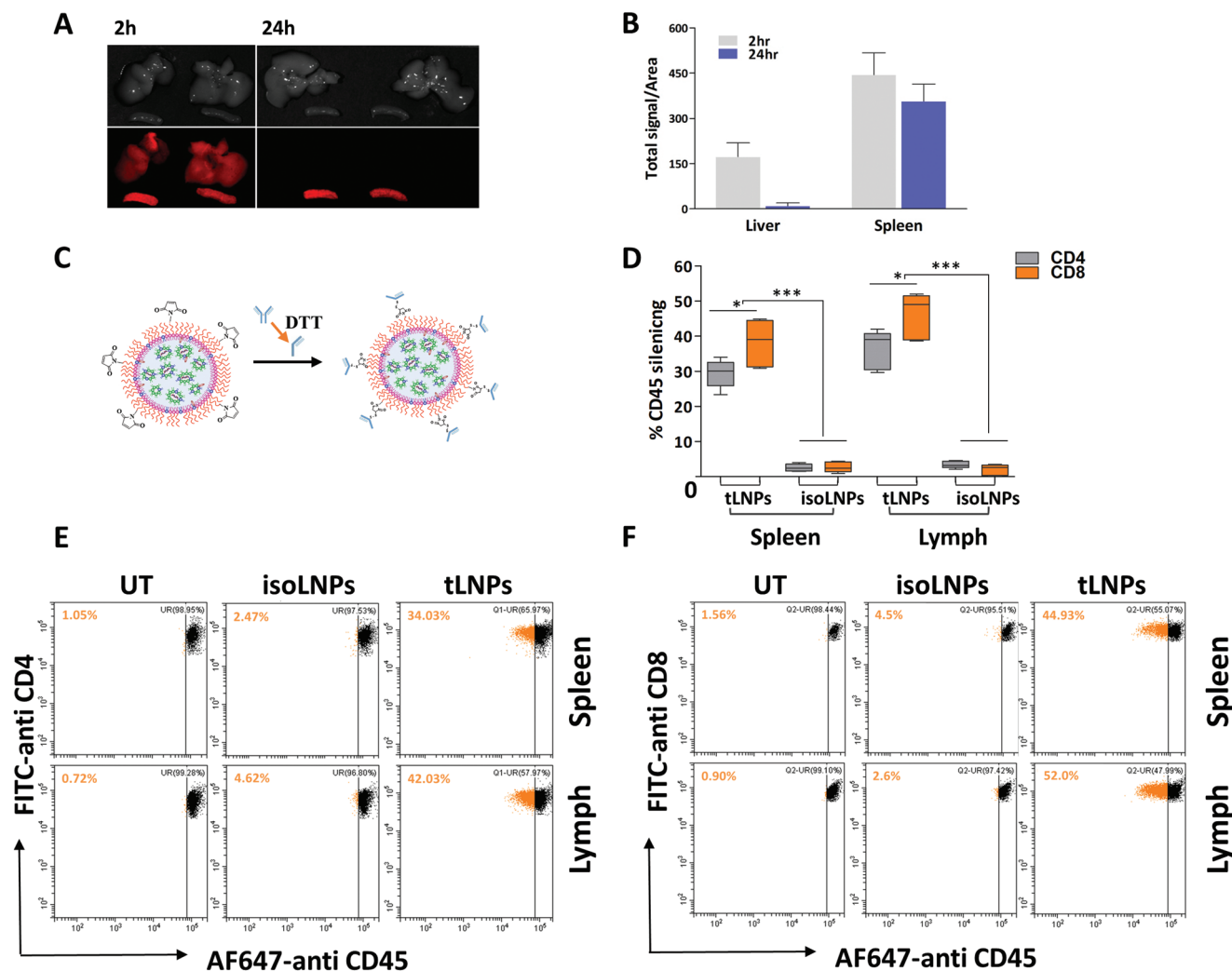


**Figure 4.** Biodistribution and in vivo gene silencing efficacy using LNPs: a) Biodistribution of Cy5-labeled lipid-10-based LNPs 2 h and 24 h post IV administration; b) analysis of the total Cy5 fluorescence signal in the liver and spleen (average  $\pm$ SD,  $n = 3$ /group, two independent experiments); c) schematic illustration of tLNP synthesis.; mice were administrated intravenously with tLNPs or isotype controlled matched-LNPs. d) Analysis of in vivo CD45 silencing in CD4<sup>+</sup> and CD8<sup>+</sup> lymphocytes by either tLNPs or isoLNPs; e, f) dot blot analysis of CD45 downregulation by flow cytometry in: e) CD4<sup>+</sup> lymphocytes; f) CD8<sup>+</sup> lymphocytes ( $n = 5$ /group, results are average  $\pm$ SD, two independent experiments,  $***p < 0.005$  isotype versus tLNPs;  $*p < 0.05$  CD4 versus CD8 of tLNPs, (two-sided student's T-test).

was attributed to the cells that are internalizing LNPs.<sup>[16]</sup> This specific population of lymphocytes has remained unknown and is currently under additional investigation. To demonstrate the linker effect on gene silencing, we further tested the gene silencing efficacy of tLNPs containing either lipid 2 (hydrazine linker) or lipid 6 (hydroxylamine) in lymphocytes. Lipid-2 tLNPs has no effect on gene silencing, whereas lipid-6 tLNPs showed significant gene silencing in lymphocytes (Figure S9, Supporting Information). These results demonstrated that ethanolamine and hydroxylamine linkers are more efficient dominators compared to hydrazine linkers in gene silencing. These results are supported by previous work demonstrating that LNPs showing surface  $pK_a$  value of 5.5 to 7.0 exhibiting efficient in vivo gene silencing.<sup>[8]</sup> We measured the  $pK_a$  values of lipid-2, lipid-6, lipid-8, and lipid-10 LNPs (Figure S8, Supporting Information). Except for hydrazine

linker containing lipid-2 LNPs, the active lipids (lipids 6, 8, and 10) exhibited  $pK_a$  values of 6.2–6.5.

Very recently, LNPs comprising of ionizable lipids were screened for gene silencing efficacy using a DNA barcode system. Some of these lipids showed gene silencing in T lymphocytes without any active targeting. Nevertheless, silencing efficacy was not substantial enough to silence stable genes like pan leukocyte marker CD45.<sup>[21]</sup>

Apart from efficient gene silencing capabilities of the newly synthesized lipids, it is important to avoid immune activation and toxicity for the use of these lipids in future clinical settings. To this end, we have evaluated the liver toxicity and cytokine secretion of few selected LNPs formulations. We have chosen lipids 2, 6 and 13 apart from lipids 8 and 10 as a characteristic structure for the linker effect and acid labile-branched lipids. As shown in Figure 5a,b, liver enzymes were transiently elevated

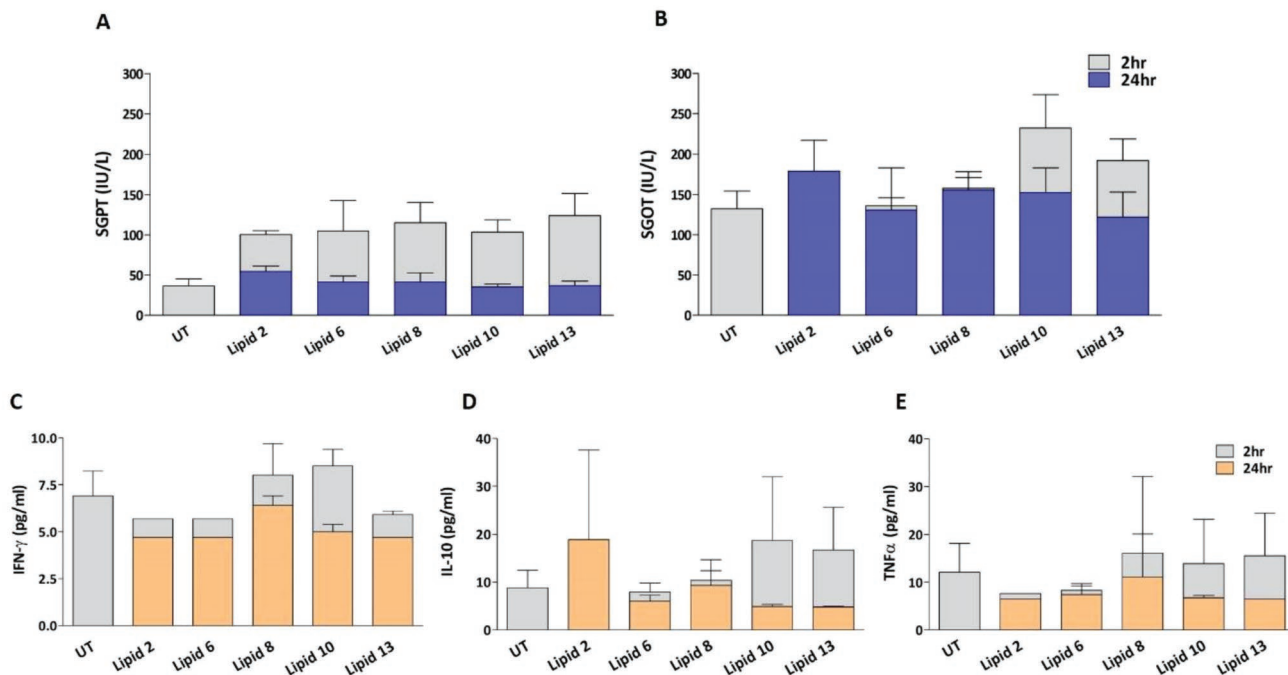


**Figure 5.** The LNPs based on the new lipids do not activate the immune system or trigger liver enzymes release. LNPs were intravenously administered into mice at 1 mg/kg siRNA dose. Blood was collected at 2 h and 24 h postinjection and analyzed for liver enzymes release (a,b) and cytokines expression (c–e). (UT: untreated; average  $\pm$  SD,  $n = 5$ ).

2 h post-LNPs administration to acceptable levels and went down back to basal levels 24 h post-administration. We further analyzed cytokine secretion, as shown in Figure 5c–e. The LNPs did not trigger any significant levels of cytokine elevation in mice compared to untreated mice. The levels of pro-inflammatory as well as anti-inflammatory cytokines were normal compared to untreated mice demonstrating the safe use of these LNPs for further exploration in clinical translation. Other cytokine levels, blood cell count, and biochemistry measurements following LNPs administration are included in the Supporting Information (Figure S11, Table S1, and Table S2).

In conclusion, we have designed and synthesized novel ionizable lipids based on the linkers ethanolamine, hydrazine, and hydroxylamine for effective gene silencing in hard-to-transfect leukocyte subsets. The new lipids were shown to efficiently silence genes of interest *in vitro* in multiple myeloma cells and *in vivo* in primary lymphocytes. Despite the headgroup effect on the biodistribution profile, hydroxylamine and ethanolamine linkers are more efficient in gene silencing compared to hydrazine linkers. In addition, no major toxic events and immune activation were observed for the lipids with different linkers. Taken together, these results suggest that these novel lipids could open new avenues for delivering RNA payloads to specific cell types and ultimately could be used in clinical practice.

## Experimental Section

All the chemicals were obtained from Sigma Aldrich chemicals unless mentioned. Linoleic acid was obtained from TCI chemicals, Belgium. 3-(4-Methylpiperazin-1-yl) propanoic acid were obtained from Santa

Cruz biotechnology, USA. Monoclonal antibodies: Alexa Fluor 488 antihuman/mouse CD44 (clone IM7), FITC antimouse CD8 (clone 5H10-1), PerCP antimouse CD3 (clone 145-2C11), PE antimouse CD19 (clone 6D5) and PE antimouse CD4 (clone GK1.5) were purchased from Biolegend (CA, USA). Antimouse FIB (clone FIB504) and Rat IgG2a isotype (clone 2A3) were purchased from Biorcell (NH, USA).

Lipids: Cholesterol, DSPC, and DSPE PEG-Mal were obtained from Avanti polar lipids, USA. The ionizable lipid Dlin-MC3-DMA was synthesized according to the previously described method.<sup>[10]</sup> Chemically modified siRNAs against PLK1, NC5, and Cy5-NC5 obtained from IDT.

LNPs were prepared by using microfluidic micro mixture (Precision NanoSystems, Vancouver, BC) as previously described.<sup>[16]</sup> Briefly, one volume of lipid mixtures (ionizable lipid, DSPC, cholesterol, and DMG-PEG at 50:10:38.5: 1.5-mole ratio) in ethanol and three volumes of siRNA (1:16 w/w siRNA to lipid) containing acetate buffer solutions were mixed through the micromixer at a combined flow rate of 12 mL min<sup>-1</sup>. In order to synthesize tLNPs, DSPE-PEG-Mal (0.5 mol%) was included during the synthesis. The resultant mixture was dialyzed against phosphate-buffered saline (PBS) (pH 7.4) for 16 h to remove ethanol. For Cy5-labeled particles, 50% Cy5-labeled nontargeted siRNA was used and the amount of siRNA encapsulated was calculated by ribogreen assay as mentioned elsewhere.

Integrin  $\beta 7$  IgG (clone FIB504) or Isotype mAbs (clone X63) were reduced with  $3 \times 10^{-3}$  M dithiothreitol (DTT) for 30 min at room temperature. DTT was removed by using 7K cut off Zeba spin desalting columns (Thermo, USA) according to manufacturer protocol. Maleimide functionalized LNPs were added and incubated for 1 h at room temperature and overnight at 4 °C. To remove unconjugated antibody, LNPs were loaded on sepharose CL-4b beads and purified by gel filtration chromatography using phosphate buffer saline as a mobile phase. LNP fractions were collected and concentrated by 100K Amicon tubes (Millipore).

The size and zeta potential of LNPs-siRNA were measured by dynamic light scattering using Malvern Nano ZS Zetasizer (Malvern Instruments Ltd, Worcestershire, UK). Size and zeta potential measurements were performed in PBS (pH 7.4) and water, respectively.

A drop of the aqueous solution containing LNPs (with or without mAbs) was placed on the carbon-coated copper grid and dried. The morphology of LNPs was analyzed by a Joel 1200 EX (Japan) transmission electron microscopy.

Vitrified LNP samples were prepared at a controlled temperature and at water saturation as previously described.<sup>[22]</sup> Cryo-samples were examined using a Talos F200C (FEI) using a Gatan 626 cryo holder maintained at below  $-170\text{ }^{\circ}\text{C}$ . Images were recorded on a Falcon 3 direct electron detector (Thermo Fisher Scientific) at low-dose conditions.

Multiple myeloma cells were treated with either siPLK-LNPs or siLUC-LNPs for 72 h. Cells were then collected and analyzed for viability (XTT assay), apoptosis (Annexin-PI assay), and mRNA levels (qPCR).

U266 cells (ATCC) were incubated with lipid-8 or lipid-10 LNPs for 4 h. Cells were then washed with PBS twice and fixed with 4% PFA (paraformaldehyde) for 30 min at room temperature. Cells were washed twice with PBS and blocked with 2% BSA for 1 h at room temperature. Cells were washed and further incubated with antimouse/human CD44-Alexa Fluor488 antibody (Bioegend 103016) at a dilution of 1:100 for 1 h followed by the nucleus staining with Hoechst. Imaging was performed using a Leica SP8 confocal microscope.

8–6 week old C57BL6/J mice were obtained from the Animal Breeding Center, Tel Aviv University (Tel Aviv, Israel). All animal protocols were approved by the Tel Aviv Institutional Animal Care and Use Committee. Mice were maintained and treated according to the National Institutes of Health guidelines. tLNPs or isotype LNPs containing siRNA against CD45 were injected intravenously on day 1 and day 3 at  $1\text{ mg/kg}$  siRNA. Mice were euthanized after 5 days and organs were collected for further analysis.

LNPs were injected intravenously into C57BL6/J mice. Blood was collected 2 h and 24 h after injection. The serum was separated and stored at  $-80\text{ }^{\circ}\text{C}$  prior to cytokine analysis. Hematology and cytokine analysis were done at AML central lab services and Pharmaseed preclinical CRO, Israel, respectively.

The surface  $pK_a$  values of LNPs were determined using TNS assay as described previously.<sup>[15]</sup> Briefly, buffer solutions with varying pH values ranging from 2.0 to 10.0 were prepared using  $20 \times 10^{-3}\text{ M}$  sodium phosphate,  $25 \times 10^{-3}\text{ M}$  citrate,  $20 \times 10^{-3}\text{ M}$  ammonium acetate and  $150 \times 10^{-3}\text{ M}$  NaCl. LNPs and 2-(*p*-toluidinyl)naphthalene-6-sulfonic acid (TNS, Sigma Aldrich) was diluted into these different pH solutions at a final concentration of 20 and  $6 \times 10^{-3}\text{ M}$ , respectively in a 96 well black plates. Fluorescence intensity was read on plate reader at an excitation of 322 nm and an emission of 431 nm. The fluorescence signal at pH 4.6 was taken as 100% and the  $pK_a$  values were calculated as the pH corresponding to 50% LNP protonation.

LNPs were incubated for 24 h with PBS with or without fetal calf serum (10% or 50%) in  $37\text{ }^{\circ}\text{C}$ , followed by treatment with or without Triton X-100 (0.5%). LNPs were then resolved on agarose gel (2%) and visualized by bioimaging system (MiniLumi, DNR).

## Supporting Information

Supporting Information is available from the Wiley Online Library or from the author.

## Acknowledgements

S.R., I.H., and R.P. contributed equally to this work. This work was supported in part from the Momentum fund at Tel Aviv University and the Lewis Trust for blood cancer awarded to D.P.

## Conflict of Interest

D.P. has a financial interest in Quiet Therapeutics and ART Biosciences. D.P. and S.R. filed two patent applications regarding this work. The rest of the authors declare no competing financial interest.

## Keywords

gene silencing, lipid nanoparticles, synthetic small interfering RNA, targeted delivery, T-lymphocytes

Received: September 18, 2019

Revised: December 4, 2019

Published online: January 30, 2020

- [1] J. Lieberman, *Nat. Struct. Mol. Biol.* **2018**, *25*, 357.
- [2] K. A. Whitehead, R. Langer, D. G. Anderson, *Nat. Rev. Drug Discovery* **2009**, *8*, 129.
- [3] A. Fire, S. Xu, M. K. Montgomery, S. A. Kostas, S. E. Driver, C. C. Mello, *Nature* **1998**, *391*, 806.
- [4] S. Weinstein, D. Peer, *Nanotechnology* **2010**, *21*, 232001.
- [5] S. Ramishetti, D. Peer, *Adv. Drug Delivery Rev.* **2019**, *141*, 55.
- [6] S. Ramishetti, D. Landesman-Milo, D. Peer, *J. Drug Targeting* **2016**, *24*, 780.
- [7] R. Srinivas, S. Samanta, A. Chaudhuri, *Chem. Soc. Rev.* **2009**, *38*, 3326.
- [8] S. Rietwyk, D. Peer, *ACS Nano* **2017**, *11*, 7572.
- [9] S. C. Semple, A. Akinc, J. Chen, A. P. Sandhu, B. L. Mui, C. K. Cho, D. W. Sah, D. Stebbing, E. J. Crosley, E. Yaworski, I. M. Hafez, J. R. Dorkin, J. Qin, K. Lam, K. G. Rajeev, K. F. Wong, L. B. Jeffs, L. Nechev, M. L. Eisenhardt, M. Jayaraman, M. Kazem, M. A. Maier, M. Srinivasulu, M. J. Weinstein, Q. Chen, R. Alvarez, S. A. Barros, S. De, S. K. Klimuk, T. Borland, V. Kosovrasti, W. L. Cantley, Y. K. Tam, M. Manoharan, M. A. Ciufolini, M. A. Tracy, A. de Fougères, I. MacLachlan, P. R. Cullis, T. D. Madden, M. J. Hope, *Nat. Biotechnol.* **2010**, *28*, 172.
- [10] M. Jayaraman, S. M. Ansell, B. L. Mui, Y. K. Tam, J. Chen, X. Du, D. Butler, L. Eltepu, S. Matsuda, J. K. Narayanannair, K. G. Rajeev, I. M. Hafez, A. Akinc, M. A. Maier, M. A. Tracy, P. R. Cullis, T. D. Madden, M. Manoharan, M. J. Hope, *Angew. Chem., Int. Ed. Engl.* **2012**, *51*, 8529.
- [11] G. Sahay, W. Querbes, C. Alabi, A. Eltoukhy, S. Sarkar, C. Zurenko, E. Karagiannis, K. Love, D. Chen, R. Zoncu, Y. Buganim, A. Schroeder, R. Langer, D. G. Anderson, *Nat. Biotechnol.* **2013**, *31*, 653.
- [12] D. Adams, A. Gonzalez-Duarte, W. D. O'Riordan, C. C. Yang, M. Ueda, A. V. Kristen, I. Tournev, H. H. Schmidt, T. Coelho, J. L. Berk, K. P. Lin, G. Vita, S. Attarian, V. Plante-Bordeneuve, M. M. Mezei, J. M. Campistol, J. Buades, T. H. Brannagan, 3rd, B. J. Kim, J. Oh, Y. Parman, Y. Sekijima, P. N. Hawkins, S. D. Solomon, M. Polydefkis, P. J. Dyck, P. J. Gandhi, S. Goyal, J. Chen, A. L. Strahs, S. V. Nochur, M. T. Sweetser, P. P. Garg, A. K. Vaishnav, J. A. Gollob, O. B. Suhr, *N. Engl. J. Med.* **2018**, *379*, 11.
- [13] M. A. Maier, M. Jayaraman, S. Matsuda, J. Liu, S. Barros, W. Querbes, Y. K. Tam, S. M. Ansell, V. Kumar, J. Qin, X. Zhang, Q. Wang, S. Panesar, R. Hutabarat, M. Carioto, J. Hettlinger, P. Kandasamy, D. Butler, K. G. Rajeev, B. Pang, K. Charisse, K. Fitzgerald, B. L. Mui, X. Du, P. Cullis, T. D. Madden, M. J. Hope, M. Manoharan, A. Akinc, *Mol. Ther.* **2013**, *21*, 1570.
- [14] A. Akinc, W. Querbes, S. De, J. Qin, M. Frank-Kamenetsky, K. N. Jayaprakash, M. Jayaraman, K. G. Rajeev, W. L. Cantley, J. R. Dorkin, J. S. Butler, L. Qin, T. Racie, A. Sprague, E. Fava, A. Zeigerer, M. J. Hope, M. Zerial, D. W. Sah, K. Fitzgerald, M. A. Tracy, M. Manoharan, V. Koteliansky, A. Fougères, M. A. Maier, *Mol. Ther.* **2010**, *18*, 1357.
- [15] J. Heyes, L. Palmer, K. Bremner, I. MacLachlan, *J. Controlled Release* **2005**, *107*, 276.

- [16] S. Ramishetti, R. Kedmi, M. Goldsmith, F. Leonard, A. G. Sprague, B. Godin, M. Gozin, P. R. Cullis, D. M. Dykxhoorn, D. Peer, *ACS Nano* **2015**, 9, 6706.
- [17] R. Kedmi, N. Veiga, S. Ramishetti, M. Goldsmith, D. Rosenblum, N. Dammes, I. Hazan-Halevy, L. Nahary, S. Leviatan-Ben-Arye, M. Harlev, M. Behlke, I. Benhar, J. Lieberman, D. Peer, *Nat. Nanotechnol.* **2018**, 13, 214.
- [18] Z. R. Cohen, S. Ramishetti, N. Peshes-Yaloz, M. Goldsmith, A. Wohl, Z. Zibly, D. Peer, *ACS Nano* **2015**, 9, 1581.
- [19] L. M. Kranz, M. Diken, H. Haas, S. Kreiter, C. Loquai, K. C. Reuter, M. Meng, D. Fritz, F. Vascotto, H. Hefesha, C. Grunwitz, M. Vormehr, Y. Husemann, A. Selmi, A. N. Kuhn, J. Buck, E. Derhovannessian, R. Rae, S. Attig, J. Diekmann, R. A. Jabulowsky, S. Heesch, J. Hassel, P. Langguth, S. Grabbe, C. Huber, O. Tureci, U. Sahin, *Nature* **2016**, 534, 396.
- [20] D. Peer, *J. Controlled Release* **2010**, 148, 63.
- [21] M. P. Lokugamage, C. D. Sago, Z. Gan, B. R. Krupczak, J. E. Dahlman, *Adv. Mater.* **2019**, 31, 1902251.
- [22] D. Danino, *Curr. Opin. Colloid Interface Sci.* **2012**, 17, 316.